2023 IEEE Power & Energy Society General Meeting (PESGM) | 978-1-6654-6441-3/23/$31.00 ©2023 IEEE | DOI: 10.1109/PESGM52003.2023.10252578

Measurement-Based Voltage Control Coordinating Inverter-Based Resources and Traditional Resources - New York State Grid Case Study

Chengwen Zhang[1], Yi Zhao[1], Yilu Liu[1,2]
1. The University of Tennessee, Knoxville, TN, USA
2. Oak Ridge National Laboratory, Oak Ridge, TN, USA
czhang70@vols.utk.edu
{yzhao77, liu}@utk.edu

Lin Zhu[3], Evangelos Farantatos[3], Aboutaleb Haddadi[3], Mahendra Patel[3],
3. Electric Power Research Institute, Palo Alto, CA, USA
{lzhu, efarantatos, ahaddadi, mpatel}@epri.com

Atena Darvishi[4], Hossein Hooshyar[4]
4. New York Power Authority White Plains, NY, USA
{atena.darvishi, hossein.hooshyar}@nypa.gov

***Abstract*—Inverter-based resources (IBRs) are being increasingly integrated into power systems around the world. While they may pose a challenge to power grids due to inherent volatility, they can be used as a voltage control resource due to their control flexibility. By utilizing this control flexibility combined with the increasingly available synchronized measurement and communication infrastructure of modern power systems, this paper proposes a measurement-based voltage control scheme that coordinates IBRs with traditional resources such as synchronous generators and Flexible AC Transmission Systems (FACTS) devices for voltage control. The integration of real-time synchronized measurements allows the control scheme to provide a robust performance against varying operating conditions, modeling uncertainties, and load variations. The control scheme allows flexible coordination of various voltage control resources by configuring parameter combinations. The effectiveness and performance of the proposed controller have been validated using a hardware-in-the-loop (HIL) platform.**

***Index Terms*—voltage control, inverter-based resources, synchrophasor measurement, coordinated control.**

I. Introduction

As power systems around the world are seeing rapid integration of inverter-based resources (IBRs), the increasing volatility in generation and load results in voltage profiles that are becoming challenging for system operators. Traditional voltage control strategies utilize generator excitation control, transformer tap changing, static var compensation (SVC), and other FACTS devices to contain voltage fluctuations [1]. The optimal set points of these resources can be obtained by solving optimal reactive power flow [2, 3]. However, effective scheduling and control of these resources rely heavily on the accuracy of power system models. With the increasingly high penetration of IBRs, this becomes more demanding because of the increased difficulty in forecasting.

With the increasing deployment of synchronized measurement devices and communication facilities, it is becoming feasible to design and implement measurement-based voltage control schemes that take advantage of real-time measurement feedback to reduce the dependency on power system models and load/renewable forecasting. At the same time, the IBRs where the aforementioned challenges originated, can be actually integrated into control schemes as an important part of the voltage regulating resources.

Two critical barriers need to be addressed in the development of the measurement-based voltage control scheme integrating IBRs: 1) the incorporation of real-time measurement feedback for reduced dependency on models and forecasting; 2) the coordination of the IBRs with traditional resources such as generators and SVCs. While the utilization of wide-area synchronized measurements for enhanced transmission network voltage control has been studied in [4] and [5], the methods still rely on accurate models and the need for coordinating various reactive power resources has not been addressed.

To further integrate and take advantage of synchronized measurements in voltage control, researchers proposed an approximate gradient method in [6] to formulate the real-time voltage control as an optimization problem that has the potential to be solved online with real-time measurement feedback. This enables the use of steady-state power system impedance matrices as an *approximate* agent for sensitivity analysis. The voltage control hence breaks away from the need for accurate models and forecasting. Specifically, the elements in the impedance matrices were used to derive sensitivity indices that indicate how much change can be achieved on the target bus with a certain amount of reactive power injection at buses where the actuators are located.

This work was supported by New York Power Authority (NYPA) and Electric Power Research Institute (EPRI). This work also made use of Engineering Research Center Shared Facilities supported by the Engineering Research Center Program of the National Science Foundation and Department of Energy under NSF Award Number EEC-1041877 and the CURENT Industry Partnership Program.

Based on the gradient-descent method used for voltage control, Tang, *et al.* proposed the use of heterogeneous step sizes in the search for optimal real-time control commands that flexibly coordinate different resources, where the method operates in closed-up among real-time measurements and real-time control commands [7]. It takes advantage of both the measurement feedback and the approximate power system matrices for improved resiliency against model uncertainty and noise rejection performance. The control scheme in [7] was validated by computer simulations on a three-area testing system with 9 buses in each area. Since it is based on the gradient method, the algorithm elicits low computation complexity and has the potential to be implemented on hardware for real-time execution.

As a continued effort, this paper presents the implementation and validation of the measurement-based voltage control scheme proposed in [7] on the New York state grid model. This includes the selection of measurement and actuation locations based on the real-world availability and planned deployment of resources in the New York state grid, the implementation of the voltage controller on hardware, and hardware-in-the-loop (HIL) testing of the controller for performance verification.

The rest of the paper is organized as follows: Section II discusses the design of the measurement-based voltage controller and its implementation on industry-standard embedded controller hardware. Section III presents the hardware-in-the-loop testing platform and the NY state grid model on a real-time simulator. Section IV discusses the HIL testing results, and conclusions are made in Section V.

II. Design and Implementation of the Controller

The voltage controller implemented in this paper is a measurement-based closed-loop control scheme that takes advantage of real-time synchronized measurements and flexibly coordinates IBRs with traditional resources. This section will first present the design of the control scheme and then discuss the implementation of the controller on hardware.

A. Formulation of the Control Scheme

The voltage controller operates in a closed loop between measurement feedback and control command issuance to control the resources in real time. Inside the controller, the control is formulated as an optimization problem to minimize the reactive power output dedicated to this control scheme by searching for the most efficient responses among different resources, as given in (1). The objective function also includes the penalty for constraint violations, including voltage violations and actuator capacity violations.

$$\begin{aligned} min[F_{obj}] &= \min\left[f + h_V + h_Q\right] \\ f &= (\Delta \boldsymbol{Q_c})^T \boldsymbol{R_c} (\Delta \boldsymbol{Q_c}) + \left(\Delta \boldsymbol{Q_g}\right)^T \boldsymbol{R_g} \left(\Delta \boldsymbol{Q_g}\right) + (\Delta \boldsymbol{Q_s})^T \boldsymbol{R_s} (\Delta \boldsymbol{Q_s}) \end{aligned} \tag{1}$$

where $\boldsymbol{Q_c}$ is the reactive power dispatched for voltage control from IBRs, $\boldsymbol{Q_g}$ from generators, and $\boldsymbol{Q_s}$ from SVCs ; $\boldsymbol{R_c}, \boldsymbol{R_g}, \boldsymbol{R_s}$ are weight factors that coordinate the priority of these resources in response to disturbances. The other two items in the objective function, $h_v$and h_Q, are penalty functions for voltage violations and actuator capacity violations, respectively. These violation penalties are formulated as the sum of the square of the extent of violation multiplied by a penalty factor. For example, the voltage violation penalty is formulated as:

$$\begin{aligned} h_V &= \sum_{i \in V_L} h_{Vi}(v_{li}) \\ h_{Vi} &= \begin{cases} a(v_{li} - \overline{v_{li}})^2, v_{li} > \overline{v_{li}} \\ 0, \underline{v_{li}} \le v_{li} \le \overline{v_{li}} \\ a(v_{li} - \underline{v_{li}})^2, v_{li} < \underline{v_{li}} \end{cases} \end{aligned} \tag{2}$$

where v_{li} is the voltage at load bus i to be controlled and the cap/underscore represents the upper and lower limit of the desired voltage range. Correspondingly, the penalty function h_Q is put in effect for capacity violations on the actuators.

The gradient descent method is used to facilitate the solution scheme between real-time measurement feedback and control command updates. As the controller constantly takes real-time measurement feedback and solves for the next optimal step with the gradient descent algorithm, the dependence on the accuracy of the power system model is greatly reduced. Equation (3) governs the updates made to the control commands in every control step:

$$\begin{aligned} \boldsymbol{u}(k+1) = P_U \Bigg[\boldsymbol{u}(k) - \tau \Bigg(& \left(\frac{\partial \boldsymbol{Q}}{\partial \boldsymbol{u}}\right)^T \nabla f(k) + \left(\frac{\partial \boldsymbol{v_l}}{\partial \boldsymbol{u}}\right)^T \nabla h_v(k) \\ & + \left(\frac{\partial \boldsymbol{q_v}}{\partial \boldsymbol{u}}\right)^T \nabla h_q(k) \Bigg) \Bigg] \end{aligned} \tag{3}$$

where $\boldsymbol{u}(k)$ is the control command array at time step k, $\boldsymbol{\nabla}$ is the differential operator that finds the gradient of the functions, P_U is the projection operator that projects the step of change to the control signal space, and the parameter matrix $\boldsymbol{\tau}$ contains the step sizes of the resources.

With the control scheme incorporating real-time measurements as feedback, the partial derivatives in (3) can be approximated with corresponding entries in the system impedance matrix that indicates the approximate sensitivities between the variables. This not only alleviates the computational burden but also relaxes the dependence of the control on accurate system models. With this approximation, (3) becomes:

$$\boldsymbol{u}(k+1) = P_U \left[\boldsymbol{u}(k) - \boldsymbol{\tau} \left(\Pi_1^T \nabla f(k) + \Pi_2^T \nabla h_v(k) + \Pi_3^T \nabla h_q(k) \right) \right] \tag{4}$$

More details can be found in reference [7].

B. Hardware Implementation of the Controller

The controller has been implemented on industry-standard embedded controller hardware for hardware-in-the-loop testing, which is a stepping stone for potential field deployment in the future [8]. The implemented hardware controller includes major function blocks as listed below:

- The **real-time measurement receiving block** receives real-time frequency, voltage, and power measurements from

978-1-6654-6441-3/23/$31.00 ©2023 IEEE

synchronized measurement devices in the power system through the IEEE C37.118 communication protocol.

- The **control algorithm execution block** is the hardware implementation of the gradient-descent-based control algorithm on the controller platform. The algorithm is implemented by converting MATLAB code to a form that can be executed on the hardware continuously at the time step specified by the control scheme.
- The **command issuance block** sends the control signals, including the voltage references to generator exciters and SVCs, and reactive power commands to IBRs through the IEEE 37.118 protocol.
- The **data abnormality detection and protection block** continuously monitors the data stream from the synchronized measurement devices. It triggers data abnormality protection to prevent the injection of control commands to actuators once the communication or data quality from the measurement devices becomes questionable.
- The **data conditioning block** adapts the data format such that it is suitable for real-time transmission through the communication link, feeding the controller and injection to the actuators.

These function blocks are coordinated in the hardware controller as shown in Figure 1.

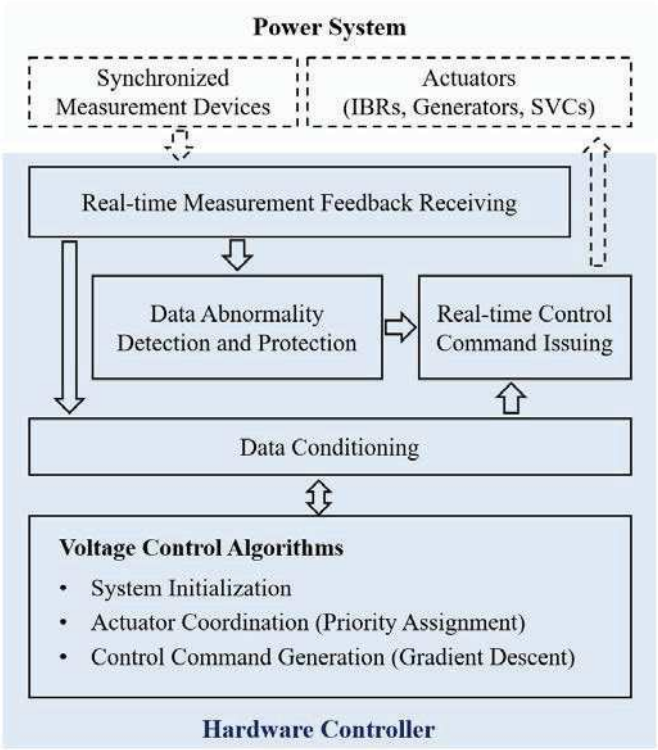

Figure 1. Structure of the hardware controller

III. The Hardware-in-the-Loop Platform

To prepare the proposed voltage controller for future field deployment, a HIL testing platform containing the NY state grid implemented on a real-time simulator is established. The hardware controller has been tested on the HIL platform for performance verification and improvement.

A. Overall Structure of the HIL Platform

The HIL testing platform simulates the NY state grid with a real-time power system simulator. Figure 2 shows the configuration that has the virtual PMUs emulated within the simulator. Both the measurement data and control commands are communicated between the simulator and the hardware controller through IEEE C37.118. The HIL testing platform is used to verify the effectiveness of the design and hardware implementation of the proposed control scheme.

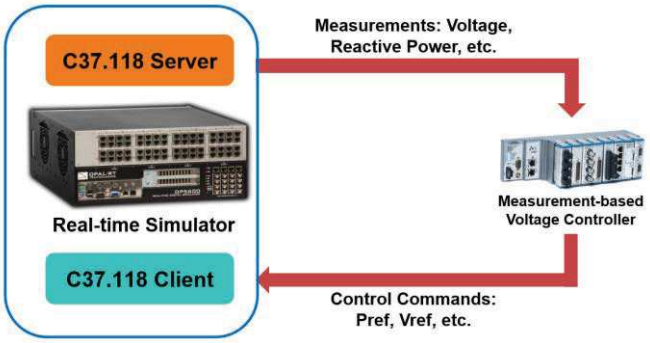

Figure 2. The hardware-in-the-loop testing platform

B. The NY State Grid Model for Real-Time Simulation

A modified 5000-bus NY state grid model is used as a case study of the measurement-based voltage control scheme on large-scale power systems. Seven onshore wind parks, one SVC, and eight synchronous generators in northern NY state are used as actuators. The one-line diagram in Figure 3 shows the location of the wind parks, SVC, and the disturbance for illustrative purposes in compliance with confidentiality requirements. While the location of the eight synchronous generators is not shown in Figure 3, they are located in the same control area. The input signals of the voltage controller are the voltage magnitude of 65 load buses in NY state, and the output signals of the controller are voltage setpoints sent to the synchronous generators/SVC and reactive power references that are sent to wind parks.

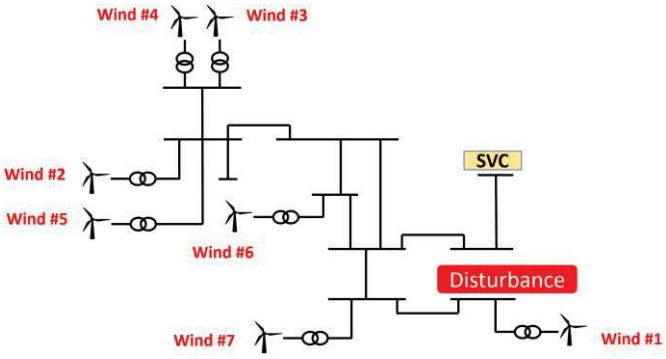

Figure 3. One-line diagram of onshore wind parks in northern NY state

The New York state grid model is implemented on the simulator for real-time simulations. The dynamic models for IBRs are built in OpenModelica [9]. Figure 4 shows the structure of the power system model implementation on the real-time simulator, including the power system solver and

978-1-6654-6441-3/23/$31.00 ©2023 IEEE

input/output ports that interface with the IEEE C37.118 communication [10].

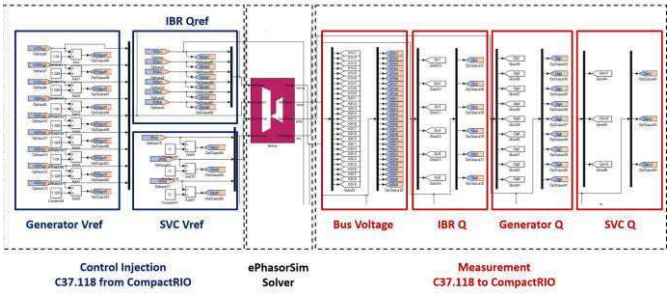

Figure 4. Implementation of the real-time simulation model

IV. HIL Testing Scenarios and Results

In the HIL testing, the voltage controller coordinates three types of reactive power resources, IBRs, generators, and SVCs. The built-in flexibility of the gradient-descent-based voltage control scheme enables a variety of coordination strategies that can be used according to the needs of application scenarios. For example, the steady-state reactive power response sharing can be coordinated by assigning different weight combinations to $\boldsymbol{R_c}$, $\boldsymbol{R_g}$, and $\boldsymbol{R_s}$ in equation (1). To coordinate the transient response, heterogeneous gradient-descent step sizes are assigned to the three types of resources by configuring the step size matrix $\boldsymbol{\tau}$ in equation (4). Two testing scenarios are presented in this section, the generator priority case where the generators take responsibility for steady-state reactive power output, and the IBR priority case where the IBRs take responsibility for the steady-state outputs. The disturbance used in both testing cases is a 300 MVar step change in reactive load.

A. Case I - Generator Priority

In this testing case, $\boldsymbol{R_g}$ in equation (1) is set to $\boldsymbol{I}$, and $\boldsymbol{R_c}$, $\boldsymbol{R_s}$ are set to $100 \cdot \boldsymbol{I}$ ($\boldsymbol{I}$ is the identity matrix) such that the generators are prioritized to maintain steady-state reactive power compensation when the objective function is minimized. The gradient-descent step sizes for the generators, IBRs, and SVCs are 0.0000025, 0.00001, and 0.0000025.

Figure 5 (a) shows load bus voltages without the voltage controller being enabled. It is noticed that there are sustained violations of the lower voltage limit of 0.95 p.u. on several load buses. By contrast, all load bus voltages were regulated back above the lower limit when the proposed controller is enabled, as shown in Figure 5 (b).

As the generators are prioritized to support the reactive power needed to regulate the voltage, the generators experienced an increase in their terminal voltages because of the control commands injected into their exciters, as shown in Figure 6 (a). The eight generators participating in the voltage control scheme increased their reactive power output by 91.5 MVar, as shown in Figure 6 (b).

As expected, the IBRs and SVCs quickly responded to the voltage transient by rapidly injecting reactive power in the first few seconds following the disturbance, as shown in Figure 7. However, they soon leveled down their output since the control prioritizes the generators to support the steady-state need for the reactive power deficiency. In this way, the IBRs, SVCs, and traditional generators are coordinated to provide satisfactory transient and steady-state reactive power regulation amid disturbances.

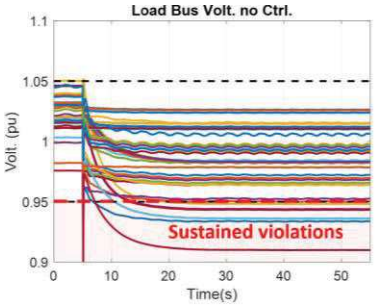

(a) Without control

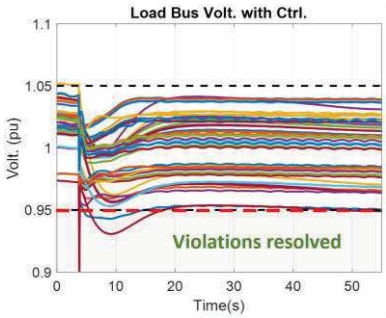

(b) With control

Figure 5. Load bus voltages with and without control (generator priority)

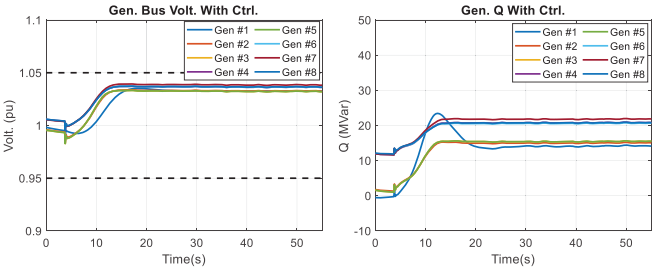

(a) Generator terminal voltage (b) Generator reactive power

Figure 6. Voltage and reactive power at participating generators

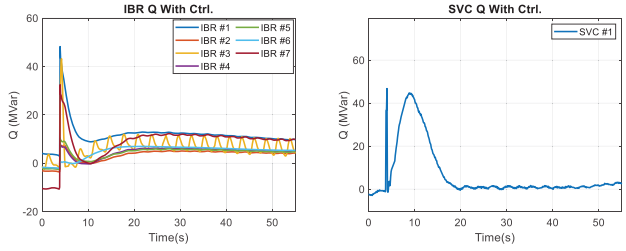

(a) IBR reactive power (b) SVC reactive power

Figure 7. Reactive power of IBRs and the SVC

B. Case II - IBR Priority

In this testing case, the IBRs are not only expected to provide the fast response during transient but also prioritized to sustain steady-state reactive power support after the disturbance. This coordination can be used when BESSs have high state-of-charge levels, or it is favorable to make use of

978-1-6654-6441-3/23/$31.00 ©2023 IEEE

spare capacity in renewable resources. The coordination parameter matrices are set as: $\boldsymbol{R_c} = \boldsymbol{I}$, $\boldsymbol{R_g} = \boldsymbol{R_s} = 100 \cdot \boldsymbol{I}$, which will allow the IBRs to take the most steady-state reactive power responsibilities when the objective function is minimized. The gradient-descent step size for the generators, IBRs, and SVCs are 0.000001, 0.00004, and 0.000001.

As shown in Fig. 8, with the fast and lasting IBR response to the voltage transients, the violations at load buses were resolved within 5 seconds, which was faster than the generator priority case.

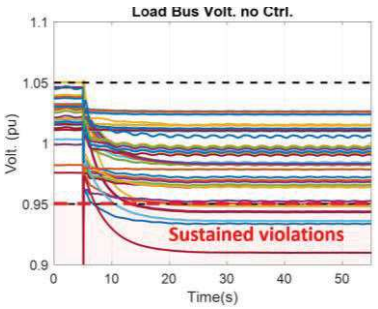

(a) Without control

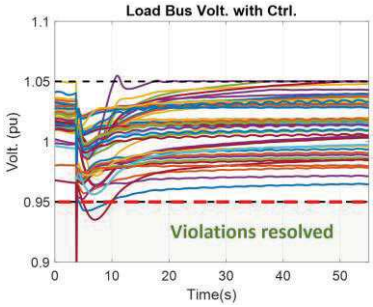

(b) With control

Figure 8. Load bus voltages with and without control (IBR priority)

As the controller puts generators at a lower priority, the changes in generator voltage and reactive power are minimal, as given in Fig. 9.

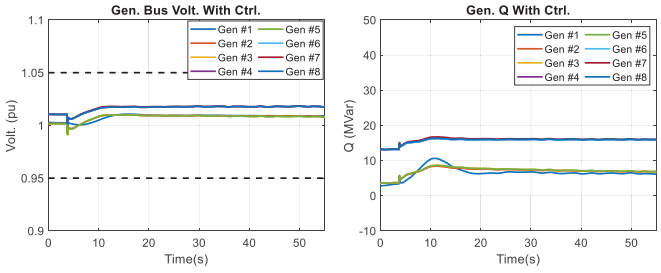

(a) Generator terminal voltage (b) Generator reactive power

Figure 9. Voltage and reactive power at participating generators

As can be seen in Figure 10, the IBRs participated in fast response instantly after the disturbance and provided a 150 MVar of steady-state reactive power support. The SVC provided a transient response to the voltage dip with minimal sustained reactive power support as expected.

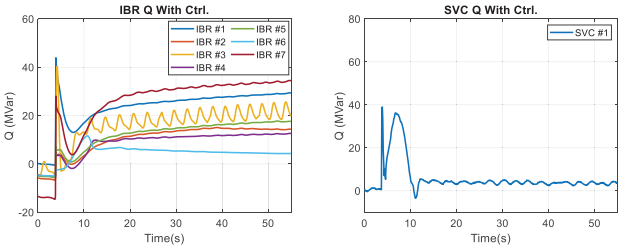

(a) IBR reactive power (b) SVC reactive power

Figure 10. Reactive power of IBRs and the SVC

V. Conclusions

This paper presented the design and implementation of a measurement-based real-time voltage control for the NY state grid utilizing existing and projected IBR resources. The control scheme took advantage of synchronized measurements and the gradient-descent algorithm to reduce its dependence on accurate system models. The control provides flexible coordination of IBRs with generators and SVCs in voltage control according to the needs of the application site. The controller has been implemented on an industry-standard, general-purpose hardware controller platform and the NY state grid has been modeled on a real-time simulator. The hardware-in-the-loop testing validated the control scheme, proved the feasibility of its hardware implementation, and prepared it for future field deployment.

In future works, the impact of communication uncertainties, including time delay, data loss, and loss of channel, will be investigated using an updated configuration of the HIL. Modules will be developed to enhance the controller's reliability under these uncertainties.

References

[1] P. Kundur, N. J. Balu, and M. G. Lauby, Power system stability and control. New York: McGraw-Hill, 1994.

[2] S. Bolognani, R. Carli, G. Cavraro, and S. Zampieri, "Distributed reactive power feedback control for voltage regulation and loss minimization," *IEEE Trans. Autom. Control*, vol. 60, no. 4, pp. 966-981, Apr. 2015.

[3] S. Corsi, M. Pozzi, C. Sabelli, and A. Serrani, "The coordinated automatic voltage control of the Italian transmission grid-part I: reasons of the choice and overview of the consolidated hierarchical system," *IEEE Trans. Power Syst.*, vol. 19, no. 4, pp. 1723-1732, Nov. 2004.

[4] H. Y. Su, F. M. Kang, and C. W. Liu, "Transmission grid secondary voltage control method using PMU data," *IEEE Trans. Smart Grid*, vol. 9, no. 4, pp. 2908-2917, July 2018.

[5] H. Y. Su and C. W. Liu, "An adaptive PMU-based secondary voltage control scheme," *IEEE Trans. Smart Grid*, vol. 4, no. 3, pp. 1514-1522, Sept. 2013.

[6] M. Colombino, J. W. Simpson-Porco, and A. Bernstein, "Towards robustness guarantees for feedback-based optimization," in *Proc. IEEE 58th Conf. Decis. Control (CDC)*, Nice, France, 2019, pp. 6207-6214.

[7] Z. Tang, E. Ekomwenrenren, J. W. Simpson-Porco, E. Farantatos, M. Patel, and H. Hooshyar, "Measurement-based fast coordinated voltage control for transmission grids," *IEEE Trans. Power Syst.*, vol. 36, no. 4, pp. 3416-3429, July 2021.

[8] "CompactRIO systems," National Instrument. [Online]. Available: https://www.ni.com/en-us/shop/compactrio.html (accessed Oct. 27, 2022).

[9] "OpenModelica," the Open Source Modelica Consortium (OSMC). [Online]. Available: https://openmodelica.org (accessed Nov. 2, 2022).

[10] "OPAL-RT real-time simulators," OPAL-RT Technologies. [Online]. Available: https://www.opal-rt.com/hardware-overview (accessed Nov.2, 2022).

978-1-6654-6441-3/23/$31.00 ©2023 IEEE